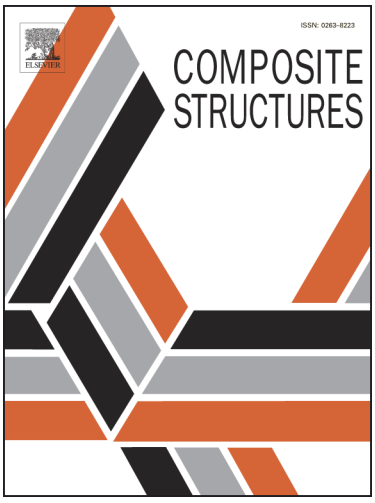

A simplified predictive approach to assess the mechanical behavior of pinned hybrid composites aged in salt-fog environment

L. Calabrese, V. Fiore

PII: S0263-8223(20)31377-5
DOI: https://doi.org/10.1016/j.compstruct.2020.112589
Reference: COST 112589

To appear in: *Composite Structures*

Received Date: 31 March 2020
Revised Date: 29 May 2020
Accepted Date: 3 June 2020

Please cite this article as: Calabrese, L., Fiore, V., A simplified predictive approach to assess the mechanical behavior of pinned hybrid composites aged in salt-fog environment, *Composite Structures* (2020), doi: https://doi.org/10.1016/j.compstruct.2020.112589

A simplified predictive approach to assess the mechanical behavior of pinned hybrid composites aged in salt-fog environment

L. Calabrese[1*] and V. Fiore[2]

[1] Department of Engineering, University of Messina

Contrada Di Dio (Sant'Agata), 98166 Messina, Italy

Email: lcalabrese@unime.it

[2] Department of Engineering, University of Palermo

Viale delle Scienze, Edificio 6, 90128 Palermo, Italy

*Corresponding Author

Abstract

Aim of this paper is to assess the predictive capabilities of a simplified theoretical approach on the failure load of aged pinned hybrid composites. In particular, the mechanical performances of glass-flax hybrid epoxy laminates exposed to salt spray fog environment, were used as input data in order to address the analytical model. Preliminarily, the relationship among mechanical performances, failure mechanisms, joint geometry and ageing time, was evaluated by double-lap joint tests on pinned samples at varying joint geometry and ageing time. The bearing and shear out limit stress of samples aged for 60 days under the salt-fog environment underwent a reduction of about 20% compared to the unaged one. Instead, the net-tension limit stress evidenced a reduction slightly above 10%. Afterward, a simplified theoretical approach, based on failure mechanisms stress limits, was proposed to forecast both joint resistance and failure mechanism occurrence. The composite degradation in a salt-fog spray environment was also taken into account in the model. The results highlight a good reliability, with an average error of about 6-8% compared to experimental results. That indicates the suitability of the proposed approach to support the long-term design of a specific pinned composite subject to critical aggressive environments.

Keywords: Bearing; salt-fog aging; flax; failure modes; hybrid composite laminates.

1 Introduction

In recent years, growing environmental awareness has favored the development of sustainable high-performance materials such as hybrid composites: i.e., polymeric materials reinforced with both natural and synthetic fibers [1,2]. Cost-effective hybrid composite laminates with structural capabilities could be acquired through an appropriate material selection. In such a context, natural and glass fibers can be considered suitable materials able to allow an effective synergy between: i) natural fibers which have numerous advantages such as biodegradability, low weight, high fatigue resistance and low cost [1] and ii) glass fibers that represent inexpensive synthetic materials having quite good ageing resistance and adequate mechanical properties [2].

However, the intrinsic structural heterogeneity of hybrid composites implies that their mechanical properties are influenced by multiple factors, such as fiber orientation and content, fiber-matrix interfacial adhesion [3]. Indeed, their design for structural applications is further constrained by the specific application conditions in which they must operate. It is quite difficult to make structural constructions or components without joining materials.

Although the joining process is a key factor in making structural composite elements, joints are usually the weakest points of the structures, thus limiting their mechanical stability [4]. In this context, geometric factors, joint set-up, stress conditions can influence the design of bearings strength and failure mode of the pinned composite joints [5].

In literature, several papers have been addressed to evaluate the mechanical response of pinned composite joints based on natural [6], synthetic [7] [8] or hybrid fibers [9] [10]. However, due to the environmental conditions in which these components operate (e.g., aircraft, building, automotive, etc.), resistance limit issues for structural design are magnified by the ageing degradation [11] [12]. This application scenario implies a premature decline in the performance of the joint, due to a progressive exposition on a severe environment, which must be properly taken into account in order to avoid unexpected mechanical failures of the structures [13] [14]. Due to the above reason, the prediction of the mechanical behavior of these pinned composite joints in critical environmental conditions is needed.

Due to the implicit difficulties to assess the local stress states that act on the composite laminate near the pin/hole contact area, the identification of effective predictive models for their practical application use is a very complex issue [15]. In this context, finite element model (FEM) has been widely used. In particular, multiple FEM approaches have been developed to predict the composite joints resistance allowing to increase the knowledge both on the mechanical behavior of these joints and on the damaging phenomena related to their fractures [16–19]. However, the use of numerical

approaches is not always compatible with the joining design needs for which an analytical model could better satisfy the balance between capacity and predictive simplicity.

An analytical method based on mass-spring model was proposed by Olmedo et al. [20] with the aim of forecasting both the stiffness and strength of bolted joints under bearing condition. Analogously, Sharos et al. [21] developed an advanced analytical model in order to predict the bearing response of multi-bolted composite joints under various load conditions. Based on the developed model, it was possible to obtain an accurate prediction of the joint mechanical response in terms of joint strength and failure condition. An analytical modified mass-spring model was proposed by Shamaei-Kashani and Shokrieh [22], who predicted the stiffness and damage initiation load of the joint by using the elastic properties of the constituents, the stacking sequence and geometrical characteristic of the composite joint as input parameters of the model. More recently a novel double-spring analytical model for hybrid GLARE joints was developed to assess and predict the mechanical properties of hybrid (bonded/bolted) GLARE joints [23].

A mono-dimensional model was proposed by Kradinov et al. [24] to evaluate the effect of laminate thickness on the strength prediction of fastened joints, by evaluating the stress state in each ply. Another method applied to assess the composite fastened joints is the progressive failure analysis [25]. Based on this approach, a progressive damage model, coupling stress distribution, failure criteria and property degradation rules can be applied to predict failure load and failure mechanism of pinned composite joints [26].

As previously clarified, several works have been developed in order to evaluate the effectiveness of analytical models in the prediction of the failure strength of pin loaded composite joints. However, these models have often a quite limited applicability due to their complexity and low adaptability. Furthermore, most of them focus interest mainly on the resistance of mechanically fastened composite joints. On the other hand, a theoretical model able to forecast the effect of ageing condition on the mechanical resistance of double-lap composite pinned joints was not yet developed, although this aspect is particularly felt theme by the industrial field. In such a context, an important aspect which has acquired increasing interest in the last few years is the assessment of fastened joints durability. It is well known that the bearing performances of composite laminates are heavy influenced by the exposition time in aggressive environments, such as marine ones [27–33].

The effect of seawater on failure behavior of mechanically-fastened, was analyzed by Sayman et al. [27] who showed that, due to 200 days seawater immersion, glass-fiber reinforced composites with stacking sequence [0/90/45/−60]s exhibit a noticeable decrease in their failure loads. Analogous results were found by Orcen et al. [29] for pinned fiberglass woven epoxy laminates. In particular,

they observed that the ageing condition influences in different way the mechanical performance degradation, as function of joint geometry configuration.

Esendemir and Cabioglu [30] evaluated the bearing strength and failure mechanism of pinned glass composite joints in several ageing conditions (i.e., cold environment, hot environment, room temperature, humid environment and seawater) showing that the different environmental conditions not affect the failure modes but have a main effect on the limit strength reduction of composite-pinned joints.

A theoretical approach aimed at integrating the knowledge related to the mechanical behavior with the degradation of the joint due to extreme environmental conditions can allow the development of sufficiently effective durability predictive models of the pinned joints [34].

Recently, Calabrese et al [35] proposed the evaluation and forecast of the failure conditions of pinned composite joints after critical environmental conditions. In particular, a topological failure map was obtained starting with simple equations of limit resistance for each specific fracture mechanism (i.e. bearing, shear out and net tension), Based on the geometric parameters (E/D and W/D are the X and Y axis of the topological map, respectively) of the pinned joint, different failure mechanisms can be discriminated [36].

In order to improve the forecasting capability of this approach, the present paper is aimed to develop a simplified predictive model able to forecast both maximum load and failure mechanism at varying ageing time in pinned composite joints. This allows to furnish added value to this analytical approach by integrating several joint information (such as durability, strength and failure conditions) while also preserving the implicit easiness and flexibility of the model. In such a context, a simplified analytical approach was proposed in order to predict the mechanical properties and failure mechanisms of pinned hybrid laminates under critical ageing conditions, preliminarily investigated in [32]. To this aim, glass-flax fibers reinforced laminates were exposed to salt-fog environment up to 60 days. Pinned samples at varying geometrical configuration (i.e., hole diameter D in the range 4 mm -10 mm and hole distance from laminate free edge E in the range 2 mm - 20 mm) were tested in double-lap configuration after 0 days (i.e., unaged), 30 days and 60 days of salt-fog exposition, respectively. Based on experimental data, a simplified theoretical approach was proposed to forecast both joint resistance and failure mechanism occurrence at varying ageing time.

2 Experimental Part

Composite panels, dimension 350 × 350 mm^2, were manufactured through vacuum-assisted resin infusion process. Two different fabrics were used as reinforcement phase: i) 2 × 2 twill weave woven flax fabric (nominal areal weight 318 g/m^2) supplied by Lineo (France) ii) plain weave

woven glass fabrics (nominal areal weight 200 g/m^2) supplied by Mike Compositi (Italy). Therefore, a hybrid composite laminate with stacking sequence (G3/F3)s (i.e., F indicates the internal flax reinforced layers and G is referred to the external glass layers). A DEGBA epoxy resin, SX8 EVO, supplied by Mates Italiana, (Italy) was used as matrix. The curing cycle, according to matrix datasheets, was constituted by a first step at 25°C for 24 h followed by a subsequent post-curing step at 50°C for 8 h.

Details of bearing test setup and hybrid laminate characteristics (i.e., fiber and void contents of the laminate, nominal thickness) are reported in our previous paper [37], and for sake of brevity they will not summarized here.

Salt-fog ageing test was performed according to the ASTM B 117 standard, by using a DCTC 600 climatic chamber (Angelantoni, Italy). In particular, the effect of the exposition time in salt-fog environment was evaluated by testing two different batches, aged for 30 and 60 days in the climatic chamber, respectively). Once reached the chosen ageing time, composite panels were extracted from the salt-fog chamber and prismatic samples with length 150 mm were cut from their center by using a band saw. Then, to avoid edge defects on the hole geometry, a preliminary undersized hole was realized in each sample by using a drilling bit and finally a mill tool was applied to obtain the desired hole diameter. With the aim of evaluating the relationship between the ageing bearing performances of the joints and their geometry, hole diameter (D) and distance between hole and laminate free edge (E) were varied to obtain pinned samples at varying W/D and E/D geometrical ratios.

Double-lap pinned joint tests were carried out to assess the bearing performances, according to ASTM D5961/D standard (procedure A). A universal testing machine Z250 (Zwick-Roell, Ulm, Germany), equipped with a 250 kN load cell, was used for the mechanical test, by setting a displacement rate equal to 0.5 mm/min.

All samples are codified by using a suffix “GFA”, “GFB”, and “GFC” depending on exposition time to salt-fog environment: i.e., 0, 30, or 60 days, respectively. In order to discriminate all joints configuration, the code was detailed with three numbers, defined as “xx-yy-zz”, related to hole diameter (D), free edge distance (E), and sample width (W) in mm, respectively. For instance, GFC-4-10-15 indicates hybrid sample exposed to salt-fog for 60 days, having D, E and W equal to 6 mm, 12 mm, and 15 mm, respectively. Failure mechanisms and local damages of fractured pinned laminates were evaluated by using a KH-8700 3D digital microscope (Hirox, Tokyo, Japan).

3 Results and Discussion

3.1 Stress-displacement curve analysis

A preliminary mechanical behavior of aged and unaged pin-loaded hybrid laminates can be assessed by evaluating load–displacement plots acquired during double-lap pinned joint tests. By considering that the effective joint resistance is mainly related to its failure load, the applied load was considered as basic parameter for the deterministic evaluation of the mechanical behavior of the joint.

3.1.1 Effect of Edge Distance, E

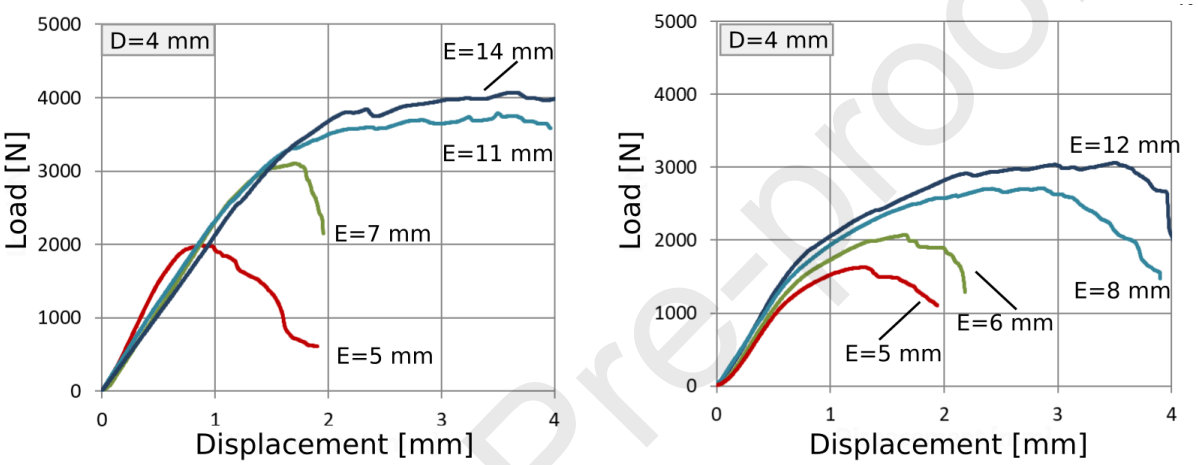

a) b)

Figure 1: Load–displacement curves for D=4 mm pinned laminates at varying E distance: a) unaged (GFA batch) and b) aged (GFC batch) samples

Typical load–displacement curves for D=4 mm pinned laminates at varying E distance for unaged GFA and 60 days aged GFC batches, as reference, are shown in *Figure 1*. It is worth noting that load–displacement trends are significantly influenced by pinned laminate configuration.

By considering unaged samples (*Figure 1*a), it can be observed that significant variations of both maximum load and displacement at failure can be found at increasing E value. The sample characterized by E=5 mm showed a maximum load of 1992 N and a displacement at maximum load of about 0.9 mm. Conversely, samples with longer edge distance (i.e., GFA_4_11_15 and GFA_4_14_15 having E equal to 11 mm and 14 mm, respectively) highlighted maximum load in the range 3700-4000 N and maximum displacement higher than 4 mm. GFA_4_5_15 and GFA_7_11_15 samples (i.e., E = 5 mm and 7 mm, respectively) exhibited an almost linear behavior until reaching maximum load. Afterward, a quite rapid decrease takes place. These samples showed a longitudinal shear out fracture mode, that extends longitudinally to load direction from the pin/hole to the sample free edge. On the other hand, samples with high E values evidenced bearing

mode as the predominant fracture mechanism. The load-displacement curve highlights a large high load plateau (with very limited load fluctuations) due to the compression collapse of the epoxy-hybrid composite laminate just behind the pin/hole contact area. *Figure 2*a shows as reference the fracture image of GFA-4-11-15 sample where a clear bearing fracture can be observed.

Similarly, the aged batch (*Figure 1*b) showed a progressive increase in maximum load and displacement at failure at increasing E value. However, noticeable differences in the mechanical behavior can be found with respect to the unaged samples.

Regardless the edge distance E, the maximum load at which the fracture of the sample occurred is considerably lower due to the exposure of the composite laminate to the salt spray environment. The effect is all the more evident the greater E distance. Furthermore, a change in the curve trend can be seen. The GFC batch shows a non-linear trend already at low load value. Samples with E = 5 mm and E = 6 mm exhibited greater displacement at break than their unaged counterparts. This could be related to a coupled action of matrix softening [38] and glass [39] and flax [40] fiber degradation which play a key role in reducing the stiffness and strength of the hybrid laminate itself [41] [42].

Vice versa, the pinned laminates with high E value (i.e., E = 12 mm) did not show an extended plateau region of the load up to large deformations. The mechanical instability of this geometric joint configuration takes place at lower load values (i.e., -21% from 3786 N to 3061 N for GFA and GFC batches, respectively). In addition, samples failed at lower displacement compared to unaged ones. This is due to the degradation action induced in the laminate by the salt spray environment, which predisposes the premature triggering of degradation phenomena in fiber, matrix and their interface [43] [44], thus leading to a premature fracture due to a mixed bearing and net tension failure mechanism. *Figure 2*b shows the fracture image of the sample GFC-4-12-15 where compressive collapse of composite laminate coupled to cross section cracks propagated orthogonally to the applied load can be observed.

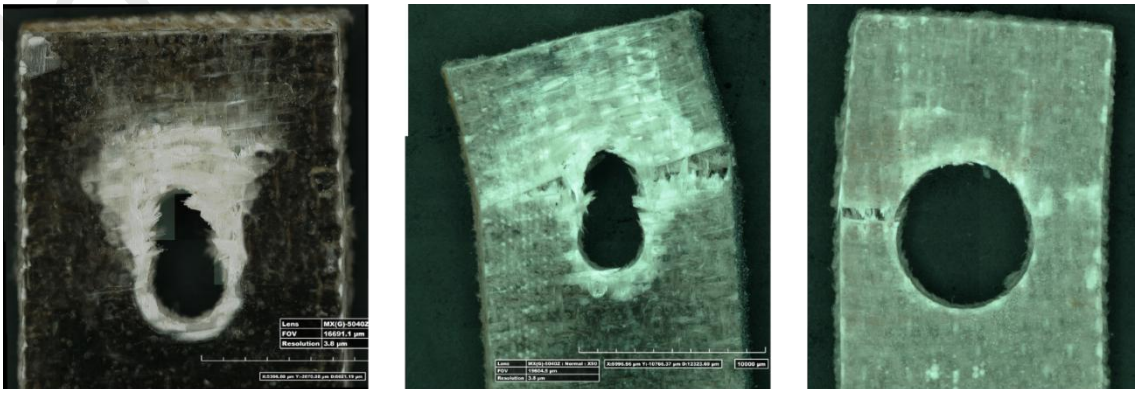

a) b) c)

Figure 2: Fracture images of (a) bearing fracture for GFA-4-11-15, (b) bearing/net tension fracture for GFC 4-12-15 c) net tension fracture for GFC-8-11-15 hybrid glass-flax samples.

3.1.2 Effect of Diameter, D

By considering unaged samples (*Figure 3*a), it is found that their load-displacement curves exhibited an initial stabilization region due to pin/hole contact adjustment [45]. Then, the curves show an almost linear trend: i.e., load increases gradually at increasing displacement until the pin-load curves reach a maximum value.

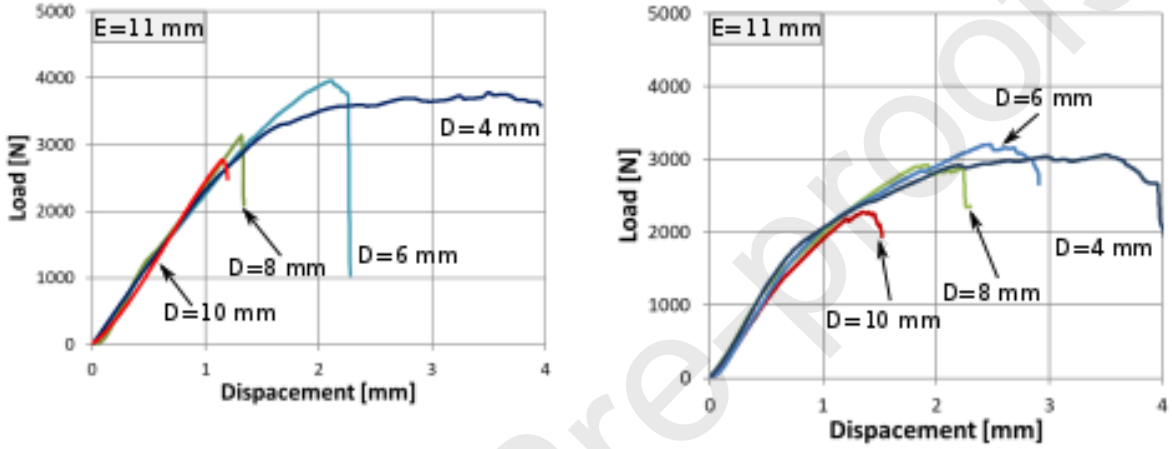

a) b)

Figure 3: Load–displacement curves for E=11 mm pinned laminates at varying hole diameter D: a) unaged (GFA batch) and b) aged (GFC batch) samples

Afterwards, the load suffered by the pinned joint decreases indicating that a relevant damage mechanism occurred. The load reduction was more sudden for all pinned samples except for the one that experienced a bearing fracture (D=4 mm). For this sample, as observed in *Figure 1*a, a load plateau before the collapse was observed. All other samples evidenced a catastrophic net-tension failure, characterized by an abrupt load drop after reaching its maximum value.

By analyzing aged GFC samples (*Figure 3*b), it is worth noting that the failure of mechanical pinned laminate occurred, prematurely, at low load values. Furthermore, the load-displacement trends exhibited a not linear behavior. A slight progressive decrease of the load slope at increasing displacement, until the maximum load value is reached, can be observed. This different mechanical behavior can be ascribed to the coupled effects of matrix softening and chemo-physical degradation phenomena that occur on the composite constituents and interfaces (i.e., water diffusion, , fiber and matrix swelling) [36].

For these joint configurations, two main failure mechanisms were observed. By progressively reducing the hole diameter a transition from dominating net-tension (*Figure 2*c) to mixed net tension -bearing fracture mode occurred (*Figure 2*a).

3.2 Failure mechanisms at varying joint geometry

These results highlight a clear correlation between the mechanical behavior and the geometry of the joint, which requires further investigation to better discriminate the laminate degradation phenomena. On such a context, further information on the damage mechanism of the pinned joints can be taken by analyzing Figure 4. These graphs showed the evolution of the maximum load (Pmax) as function of the displacement at the maximum load (ΔL@Pmax), for different values of the hole diameter D (Figure 4a-d). The marker size is linked to the E value, the distance of the hole from the edge: e.g., the larger the marker size the more distant hole is from the free edge.

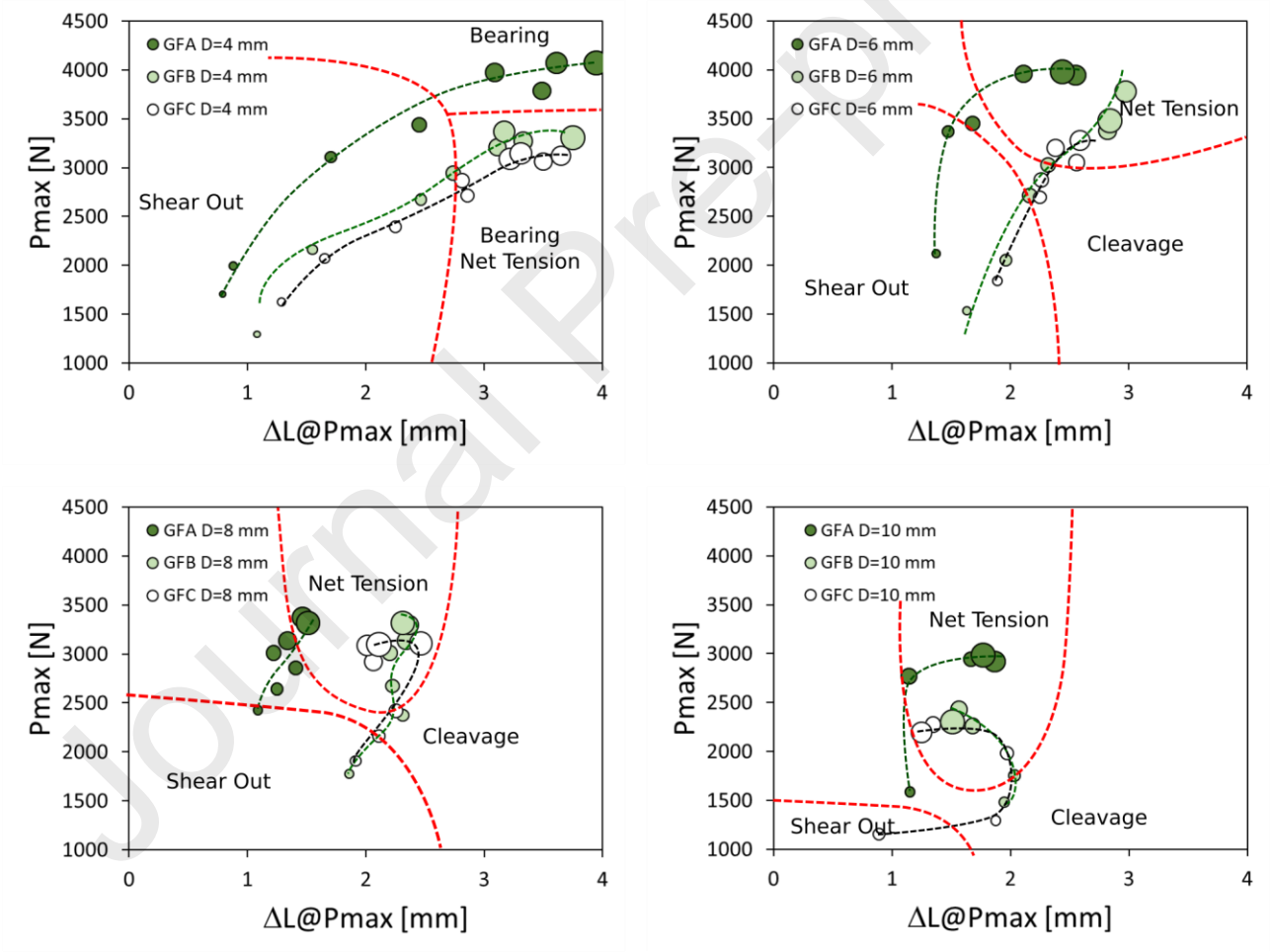

Figure 4: Maximum load (Pmax) vs displacement at maximum load (ΔL@Pmax) curves at varying diameter: a) D=4mm; b) D=6mm; c) D=8mm; d) D=10mm; for all composite batches. Marker size indicates the free edge distance E. Dotted red lines indicate occurred failure mechanism areas

Figure 4a shows results for all batches characterized by a hole diameter equal to 4 mm. It can be observed that at increasing edge distance, gradual increase of both Pmax and ΔL@Pmax occurred. For small E values, the laminates undergo a premature shear out fracture. In this region, the very limited distance behind the pin/hole suffers high stresses that trigger the activation and propagation of premature fracture by shear out mechanism. Instead, when the hole is very far from the edge (i.e., high E values), the predominant fracture mechanism becomes bearing [46]. This fracture mode, which is not catastrophic, but progressive, leads equally to a longer ΔL@Pmax and maximum load. However, a significant downward shift of the curve trend can be highlighted for GFB and GFC batches, due to exposure to the salt spray fog environment: i.e., these batches show a lower maximum load values than GFA batch. Due to wet ageing, hybrid laminate, as also shown in *Figure 1* and *Figure 3*, becomes more ductile, thus limiting the triggering of catastrophic cracks but instead stimulating, fiber/interface and delamination as dominating fracture mechanisms [47].

Further details can be argued by analyzing the trend of deformation at maximum load. For low E values (i.e., region with small size markers), just 30 ageing days implies a significant increase in displacement (i.e., curves are shifted on the right toward larger ΔL@Pmax) indicating a reduction in the overall stiffness of the pinned joint. For longer E values (i.e., region with large size markers), instead, a slight reduction in displacement is detected. This behavior is attributable to the significant reduction in the maximum load related to the loss of strength of the laminate due to ageing. Furthermore, this behavior is amplified by the failure mechanism modification. The GFA batch evidenced, at large E distance, a bearing failure mechanism. On the contrary, aged laminates (i.e., GFB and GFC batches) showed a mixed bearing/net tension fracture mechanism with the former dominating over the latter. Net tension is a sudden failure mechanism that could reduce the sample displacement before its fracture [46]. The different failure mechanism leads, therefore, to increase the differences in elastic-plastic behavior of the batches, both in Pmax and in ΔL@Pmax.

For hole diameter D larger than 4 mm, a noticeable change of the failure mechanism areas can be evidenced (Figure 4b-d). The shear out cluster progressively takes place at lower Pmax values in comparison to pinned joints having D equal to 4 mm (Figure 4a).

For a large amount of joint configuration, the net tension gradually becomes the predominant failure mechanism. For these samples, load versus deformation trends gradually undergo an increase in slope at increasing E value, differently from the trends reported in Figure 4a. This indicates that, for large hole diameters D, the hole distance from the edge E influences more significantly the maximum load than ΔL@Pmax.

This behavior is justified by the presence of a progressive bearing failure mode, taking into account the small pin diameter (i.e., D = 4 mm). Therefore, a high deformation state is required before

reaching the joint mechanical instability. On the other hand, for larger hole (i.e., D = 6 - 10 mm) the predominant fracture mechanism is the net tension. This latter, being an abrupt and catastrophic premature mechanism, is characterized by a low deformation state.

Figure 4d that shows the maximum load versus the displacement at the maximum load for samples with D = 10 mm, is particularly interesting. As attended, the exposition to salt-fog environment leads to a significant reduction in the maximum load. Furthermore, it should be noted that the GFB and GFC curves (i.e., aged samples) showed an opposite trend compared to unaged samples. This behavior can be explained considering there is also a greater predisposition of the aged pinned laminate to cleavage fracture, which is characterized by a value of ΔL@Pmax slightly longer than that found for net tension mode. This leads to an increase in deformation at maximum load for specimens that had a cleavage fracture compared to specimens that undergo premature net-tension fracture. Consequently the GFB and GFC batches, due to ageing softening of the composite laminate, at increasing E, exhibited a transition, progressively, from shear out to cleavage and finally to net tension leading to a concave curve trend.

Certainly, in this evolution of the mechanical behavior of pinned laminates, as a function of the joint geometry, a key role is provided by the ageing conditions that activate degradative phenomena precursory of premature local damage of the laminate itself.

In such a context, due to exposure in salt-fog environment, the glass-flax laminates suffered chemo-physical degradation processes that could heavily decrease their mechanical properties.

Glass fibers could suffer degradation phenomena due to water diffusion toward the matrix-glass fiber interface. In more detail, a local and slight reduction of glass fiber mechanical performances could occur due to partial dissolution of their surface [48]. However, pinned fiber glass laminates exhibit acceptable mechanical stability when exposed to salt-fog conditions, as already reported [35]. Consequently, the contribution of these fibers to the degradation of fiber reinforced composite materials can be considered very limited. Indeed, their hybridization action can, thanks to the low water interaction of glass fibers, enhance the hygrothermal stability of the natural fiber reinforced composites in severe environmental conditions [49] [50] [51].

Conversely, flax fibers show a great tendency to water absorption [52] due to their hydrophilic nature. As a consequence, such fibers suffer a progressive and relevant decrease in their mechanical performances when exposed to wet or in moisture conditions [53]. This behavior is related to the intrinsic microporous structure of the flax fibers, constituted by a complex hierarchical structure based on many cellulose micro-fibrils grouped together to form meso- or macro-fibrils [54,55]. The fibril structure acts as reinforcement, thanks to their high stiffness (i.e., elastic modulus is in the range 134 to 160 GPa [56]). Nevertheless, a significant reduction of the mechanical properties of

natural fibers occurs due to high water sorption capacity of the cellulose amorphous fraction and other polysaccharides (e.g., hemicellulose) [50]. The absorbed water molecules destroy the cellulose structure inducing a reduction in fiber strength and stiffness [57]. In addition, the presence salt in the fog (Na^+ and Cl^- ions in the aerosol) accelerates the epoxy matrix and flax fibers degradation, thus reducing the adhesive force at the fiber/matrix interface that acts as preferential pathway for the osmotic water diffusion [58] [59].

The speed up of the water diffusion at the interface, induces multiple actions: i.e., facilitates the activation of local dissolution phenomena on the fiber surface, with a consequent decrease in their mechanical properties [48] and at the same time, trigger softening phenomena of the epoxy matrix [60]. The synergistic action of these phenomena induces a fast reduction of the fiber strength leading to a relevant lowering of the tensile net tension failure stress on the aged hybrid composite laminates (already after 30 days of exposition in salt-fog environment). This also leads to a reduction of the bearing stresses for the GFB and GFC samples (i.e., -18% and -24% respectively) compared to the GFA ones.

This noticeable stress reduction occurred for hybrid pinned laminates with high E and low D values can be due to a premature tensile fracture of the pinned joint by net tension that contributes synergistically with the bearing one to the mechanical collapse of the joint.

In order to better identify the correlation between fracture mechanisms and joint geometrical configuration, a topological fracture map for the GFC hybrid laminate (i.e., aged for 60 days) at varying E/D and W/D ratios is reported in *Figure 5*. The markers were distinguished by a color according to the experimentally observed fracture mode. A simplified visual representation of fracture mechanism grouped in clusters can be identified. The transitions between failure mechanisms, red lines in Figure 5, were calculated based on a theoretical approach reported in [46].

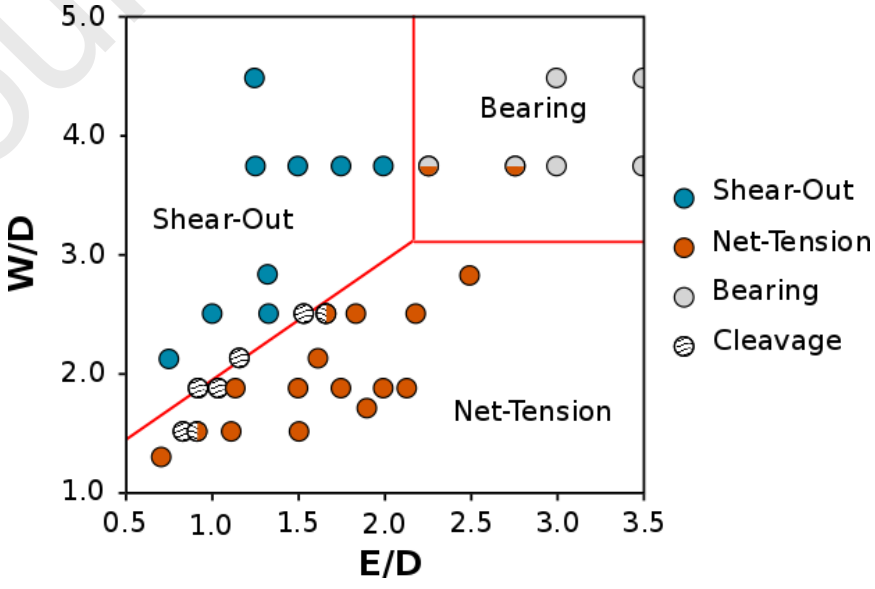

Figure 5. Failure mechanisms in E/D versus W/D plot for GFC hybrid laminate

In particular, four failure mechanism clusters can be clearly identified:

- Bearing mechanism (i.e., gray markers). It is located in the top-right corner on the map. This failure mechanism becomes the predominant one for joint geometry configurations constituted by large E/D (i.e., higher than about 2.0-2.5) and W/D (i.e., higher than about 3.0) ratios. Considering samples with fixed width W, this failure mechanism can be observed for pinned laminates with large edge distance E and small hole diameter D. For these geometrical configurations, a local laminate compression failure occurred due to the pin diameter which tends to crush the composite material.
- Net tension mechanism (i.e., brown markers). The cluster related to net tension is located in bottom side of the plot. It is the main failure mechanism for medium-low W/D ratios and preferentially high E/D ratios. Therefore, this failure mechanism happens for samples with large hole diameter and sufficiently high free edge distance. Samples with this geometry configuration are characterized by a small cross section area, orthogonal to applied load. A limited resistant cross section leads to a very intense tensile stress state. This implies a rapid and premature propagation of tensile cracks in the hybrid laminate, causing a catastrophic net-tension failure.
- Shear out mechanism (i.e., blue markers). It is the predominant failure mechanism for low E/D and preferentially high W/D ratios. Therefore, this failure mode takes place for samples with small hole dimeter D and high edge distance E. For this joint geometry configuration, the pin/ hole is located near the free sample edge, favoring the shear-out of the hybrid laminate behind the pin contact area.
- Cleavage mechanism (i.e., black wave markers). The cluster related to cleavage failure mechanism is located in the transition area between shear out and net tension zones. It is a premature catastrophic fracture due to coupled net tension and shear out crack propagation in the surround area of the hole [61] [62]. This failure mode is the predominant one for low W/D and E/D ratios. At increasing values of both of them, approaching the bearing region, the cleavage fracture is not a representative fracture mode of the joint. This behavior could be due to a complex stress state in the pinned laminate due to a combined action of tensile (net-tension), compressive (bearing) and shear (shear out) stresses that forces the mechanical joint instability for these geometric configurations, triggering premature fractures for the failure mode that, at first, takes place [36] [63].

In composite joining design, an important prerequisite is to ensure a progressive and not catastrophic damage mechanism. This allows to verify by inspection the extent of the occurring

damage and, as a consequence, to define a fracture risk index for a specific structure. This warning condition significantly contributes to increase the structural safety of the composite components, indicating the bearing failure as the suitable and favored joint design solution.

Instead, other joint failure mechanisms (i.e., cleavage, shear out and net tension) occur with a sudden load drop thus leading to a catastrophic fracture of the joint. This does not allow to identify the local damage neither to quantify the occurring failure risk. Therefore, bearing failure mode is the required failure mechanism in the joining design. Based on *Figure 5*, the bearing cluster, for 60 days aged batch, is defined by E/D and W/D ratios higher than 2.5 and 2.9, respectively. For the sake of comparison, it is worth noting that these threshold limits were found equal to 2.4 and 3.1 (i.e., E/D and W/D ratios, respectively) for unaged hybrid glass-flax pinned laminates [37]. This indicates that, due to the exposure in the salt fog spray chamber, hybrid laminates do not show a significant change of the bearing region in the failure map. Consequently, the hybridization of flax fibers with glass ones allows to improve the composites durability under salt-fog environment. Indeed, flax reinforced laminates showed a very noticeable modification of strength and failure conditions due to salt-fog exposition [36]. On the contrary, glass pinned laminates are able to suffer satisfactory stress, even after long ageing time, when bearing failure mechanism occurs [35]. This suggests that the hybridization improves the composite stability thus preserving its progressive and non-catastrophic fracture condition even after long exposure in critical environmental conditions.

This behavior allows the designer to define a univocal geometrical joint configuration guarantying that the preferred bearing failure mode will not change also after critical ageing exposition. In this context, the design must therefore be aimed at verifying the resistance limit of the joint that, instead, is strictly related to the environmental condition, as clarified in Figure 4.

3.3 Simplified predictive modelling of aged pinned joints performance

3.3.1 Limit stresses

Preliminary, a further improvement of knowledge on the mechanical performance degradation of pinned hybrid laminates due to ageing conditions can be provided by analyzing the variation of the limit strength for each fracture mechanism at varying ageing time. The limit strength for each failure mechanism can be defined as in the following equations [64] [65]:

$$\sigma_B = \frac{P_{max}}{D \cdot s} \quad \text{Eq. 1}$$

$$\sigma_{NT} = \frac{P_{max}}{(W-D) \cdot s} \quad \text{Eq. 2}$$

$$\tau_{SO} = \frac{P_{max}}{2 \cdot E \cdot s} \quad \text{Eq. 3}$$

Where σ_B, σ_{NT} and τ_{SO} are the bearing, net tension and shear out strengths, respectively. P_{max} is the maximum load experimentally obtained for a specific failure mechanism, for each joint configuration. W, D, and E are the width, the hole diameter and free edge distance, respectively. Finally, s is the thickness of the composite laminate.

Figure 6 shows the evolution of the limit stress at failure at increasing ageing time (i.e., 0, 30 e 60 ageing days for GFA, GFB and GFC batches, respectively) for the three main observed fracture mechanisms: i.e., shear out (SO), net tension (NT) and bearing (B). Each limit stress was defined as average of strength calculated, according to eq. 1-3, for samples that evidenced only a specific failure mechanism. i.e., τ_{SO} was calculated as average SO limit stress (according to eq. 3) by evaluating all samples that exhibited only shear out fracture. This average value was calculated for each batch and for each failure mechanism (i.e., shear out, bearing, net tension).

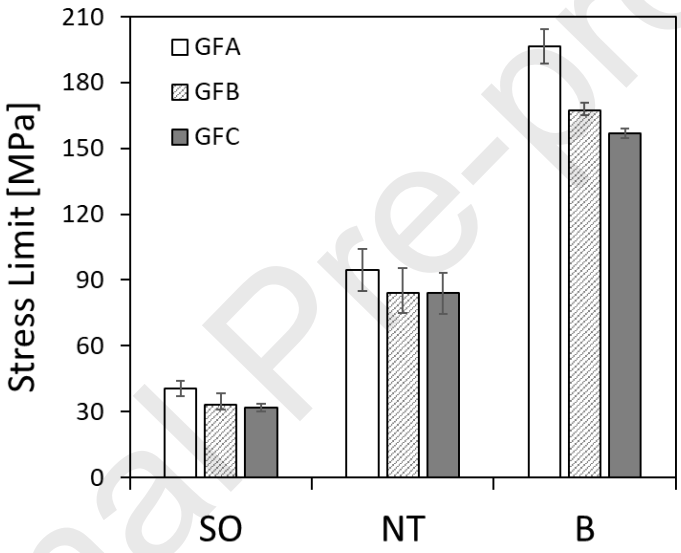

Figure 6. Bearing (B), Net tension (NT) and Shear out (SO) stress limits experimentally determined for all composite laminates

A clear relationship between limit stress and ageing time can be identified. The bearing limit stress of GFB batch (i.e., samples aged for 30 days under the salt-fog environment) underwent a reduction of about 15% compared to the GFA batch (i.e., unaged samples). This reduction, due to degradation phenomena, is amplified after 60 days of ageing: i.e., GFC batch showed a bearing limit stress of 156.9 MPa, about 20% lower than that of unaged one (i.e., 196.6 MPa). A quite similar degradation effect can be shown by evaluating the limit stress variation for SO and NT mechanism even if after 60 days of salt-fog exposition, σ_{NT} limit stress showed a lower reduction compared to other failure mechanisms: -11.3% from 94.6 MPa to 83.9 MPa for GFA and GFC batches, respectively. These results are summarized in *Table 1*.

The joint failure due to the net-tension is influenced by tensile properties of the reinforcement which plays a relevant role on the failure limit fluctuations. The structural heterogeneity of natural flax fibers, could involve a wide dispersion of their tensile properties [40]. Instead, the higher sensitivity of shear out and bearing stress limit to ageing time in comparison to net tension one can be ascribed to the local degradation phenomena occurring on hybrid laminates. It is well known that the interfacial water diffusion plays a relevant role on the triggering and propagation of degradation mechanisms [66]. This mainly stimulates a weakening of the fiber-matrix interface in addition to the matrix softening [38] [43]. It is worth noting that the shear out and bearing resistances of pinned laminates are mainly related to the fiber-matrix adhesion and matrix stiffness, respectively [67] [68]. Conversely, the tensile strength of the composite laminates greatly influences their net tension resistance [69]. Due to these reasons, it can explainable that shear out and bearing fracture are heavier influenced by the ageing time than net tension one. The still effective longitudinal strength and stiffness of glass fiber offers an acceptable stability of net-tension resistance on the hybrid flax-glass laminates, leading to a reduction of net-tension strength, induced by exposition in salt fog environment, slightly above 10%. This behavior is therefore enhanced by the hybrid nature of the fiber reinforced composite. Flax fibers suffer significantly the wet and humid environment resulting in a significant reduction of pinned joints performances [36]. Conversely, the glass fibers noticeably contribute in the tensile stability of the composite laminate thanks to their acceptable durability in salt-fog environment [35]. Glass/flax fiber hybridization, therefore, plays a key role in making the material durable and suitable in aggressive environments. At the same time, an adequate balance of performance is acquired maintaining a role of environmental sustainability in the composite laminate.

Table 1. Shear Out (SO) Net Tension (NT) and Bearing (B) stress limits and relative reduction (%) at increasing ageing time compared to GFA batch

		Stress Limit [MPa]			**Reduction [%]**		
Ageing [days]	*Batch*	**SO**	**NT**	**B**	**SO**	**NT**	**B**
0	*GFA*	40.5	94.6	196.6	0.0%	0.0%	0.0%
30	*GFB*	32.9	84.1	167.3	18.7%	11.1%	14.9%
60	*GFC*	31.8	83.9	156.9	21.5%	11.3%	20.2%

3.3.2 Simplified model description

Based on the geometrical characteristics of the joint, it is possible to theoretically forecast the occurring fracture mechanism and the related maximum load by using the relationship between bearing, net tension and shear out limit strength [64]. Defining a pinned laminate geometry configuration, based on eq. 1-3, it is possible to determine the attended maximum load if a specific failure mechanism will occur. In particular:

$$P_B = \sigma_B \cdot (D \cdot s) \qquad \textit{Eq. 4}$$

$$P_{NT} = \sigma_{NT} \cdot ((W - D) \cdot s) \qquad \textit{Eq. 5}$$

$$P_{SO} = \tau_{SO} \cdot (2 \cdot E \cdot s) \qquad \textit{Eq. 6}$$

Where P_B, P_{NT} and P_{SO} is the attended maximum load for the activation of a bearing, net tension and shear out fracture mode, respectively. The lowest value identifies the limiting failure mechanism and its related, P_{max}. Therefore, rearranging eq. 4-6, the forecasted P_{max} can be defined, evaluating the three main failure mechanisms model (coded with the acronym: 3FM model), as:

$$P_{max} = s \cdot \mathrm{D} \cdot \left\{ \begin{matrix} \alpha_B \cdot \sigma_B \\ \alpha_{NT} \cdot \sigma_{NT} \cdot (W/D - 1) \\ \alpha_{SO} \cdot \tau_{SO} \cdot (2 \cdot E/D) \end{matrix} \right\}_{min} \qquad \textit{Eq. 7}$$

Where σ_B, σ_{NT} and τ_{SO} are the bearing, net tension and shear out average strengths reported in *Table 1* for the unaged batch (GCA). Furthermore, α_B, α_{NT} and α_{SO} are corrective factors added in order to take into account the ageing effect. They can be identified as degradation index for bearing, net tension and shear out, respectively. For instance, $\alpha = 1$ indicates that no ageing effect occurred. Conversely, $\alpha = 0.8$ indicates that ageing induces a 20% performance reduction. For instance, *Table 1* reports that the GFC sample has a reduction of bearing limit stress of 20.2 %: i.e., therefore a correction factor $\alpha_B = (1 - 0.202) = 0.798$ can be obtained for this sample. In order to generalize the present approach for a generic ageing time, the correction factors have been calculated as interpolation of experimental data reported in *Table 1* as a function of the ageing time. A 2nd order polynomial regression model was applied.

$$\alpha_{SO} = 8{,}9 \cdot 10^{-5} \cdot \mathrm{t}^2 - 0.0089 \cdot \mathrm{t} + 1 \qquad \textit{Eq. 8}$$

$$\alpha_{NT} = 6{,}1 \cdot 10^{-5} \cdot \mathrm{t}^2 - 0.0055 \cdot \mathrm{t} + 1 \qquad \textit{Eq. 9}$$

$$\alpha_B = 5.3 \cdot 10^{-5} \cdot \mathrm{t}^2 - 0.0066 \cdot \mathrm{t} + 1 \qquad \textit{Eq. 10}$$

Where t is the ageing time, expressed in days. All fitting equations showed a R squared value equal to 1 indicating the goodness of the applied fitting.

For sake of clearness, the calculation steps for a reference geometry are briefly summarized. If the objective is to forecast the attended maximum load for the sample GFC-4-11-15 the eq 7 needs to be applied. The joint geometry is known. The ageing time is 60 days (GFC batch) and therefore all corrective factors are known, according to eq.8-10. Introducing the GFA stress limit for each failure mechanism (*Table 1*) the relative attended maximum load can be obtained (based on eq. 4-6). The lowest maximum load defines the joint resistance and the theoretical occurring failure mechanism (eq. 7).

3.3.3 Model validation and improvements

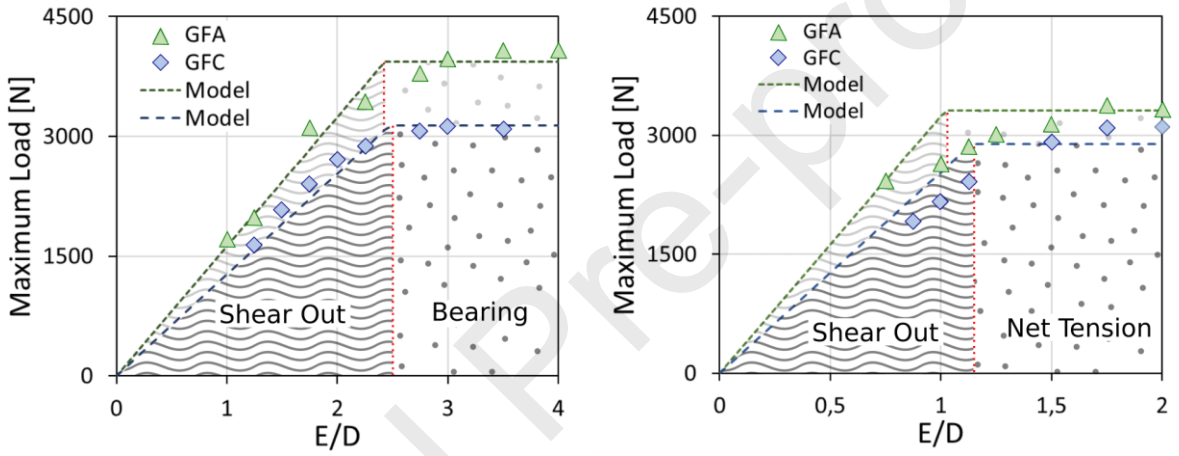

a) b)

Figure 7. Comparison of Three Failure Mechanism Model and experimental data for unaged (GFA) and aged (GFC) hybrid pinned joint: a) D = 4 mm; b) D = 8 mm.

Figure 7a shows the failure plot for unaged GFA and 60 days-aged GFC hybrid pinned joints having D equal to 4 mm. Markers represent the experimental maximum load data whereas the dotted lines are referred to theoretical failure model forecasted according to eq.7, for unaged and aged conditions.

The simplified theoretical model effectively overlaps both GFA and GFC experimental data. The transition from shear-out to bearing failure mechanism was also confirmed at about E/D=2.3-2.4. It is worth noting that, due to the exposition to salt-fog, a slight shift of E/D threshold toward higher values can be highlighted.

A larger discrepancy between experimental data and theoretical model can be observed for pinned laminate having hole diameter D equal to 8 mm, as shown in Figure 7b. A clear deviation of the

model with respect to the experimental data can be found around the fracture mechanisms transitions. This discrepancy is justified by considering that the model does not include the cleavage fracture, which was instead experimentally found for pinned laminates of these batches. The combined action of the stresses induced by shear-out and net-tension involves a reduction of the critical failure load compared to the theoretical model, which slightly overestimates or underestimates the maximum resistance of the joint in this region. Samples with D equal to 8 mm showed a larger cleavage fracture area, in comparison to the geometrical configuration with D = 4 mm (see Figure 4). This lead to an acceptable, but not optimal, prediction of the critical maximum load for this joint configuration.

However, if a further model refinement and improvement is required, due to stringent design constraints, a possible strategy could be to integrate the contribution of cleavage mode. By considering that cleavage fracture is due to a synergistic action of net-tension and shear out mechanisms, the required variables for its calculation are the coupling of: i) net section dimension (W - D), ii) edge distance, E iii) net tension and shear out strength. A simplified equation to predict the maximum cleavage load, P_{CL}, can be [70]:

$$P_{CL} = C_{CI} \cdot \left(\frac{P_{NT}+P_{SO}}{2}\right) = C_{CI} \cdot \left[s \cdot \left(\frac{\sigma_{NT}\cdot(W-D)+\tau_{SO}\cdot(2\cdot E)}{2}\right)\right] \qquad Eq.\ 11$$

Where C_{CI} is a coupling index, which was added to take into account the synergistic action of net-tension and shear out contribute and experimentally quantified as 0.83. By adding this equation in eq. 7, it was possible to rearrange the forecasting model. The new model results, that consider also the cleavage mode (Four Failure Mechanisms model – 4FM Model), are in good agreement to the experimental one, both in terms of failure mechanism and maximum load. The good predictive capacity of the model toward the occurred fracture mechanism can be assessed by comparing the theoretical results (*Figure 8*) with the experimental (*Figure 4*).

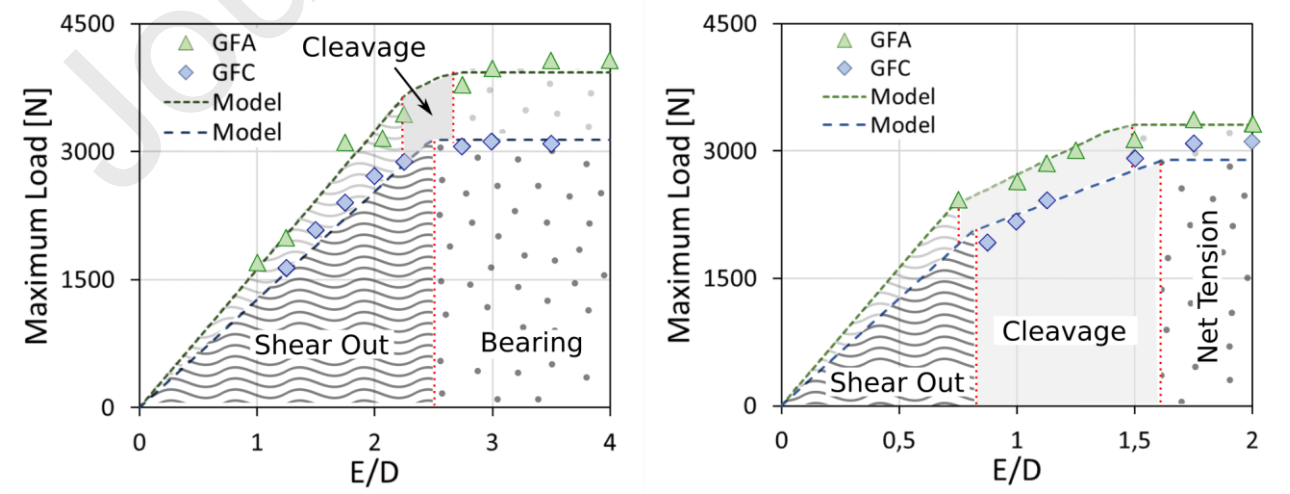

a) b)

Figure 8. Comparison of Four Failure Mechanism Model and GFC experimental data for unaged (GFA) and aged (GFC) hybrid pinned joint with a) D=4 mm. and b) D=8 mm.

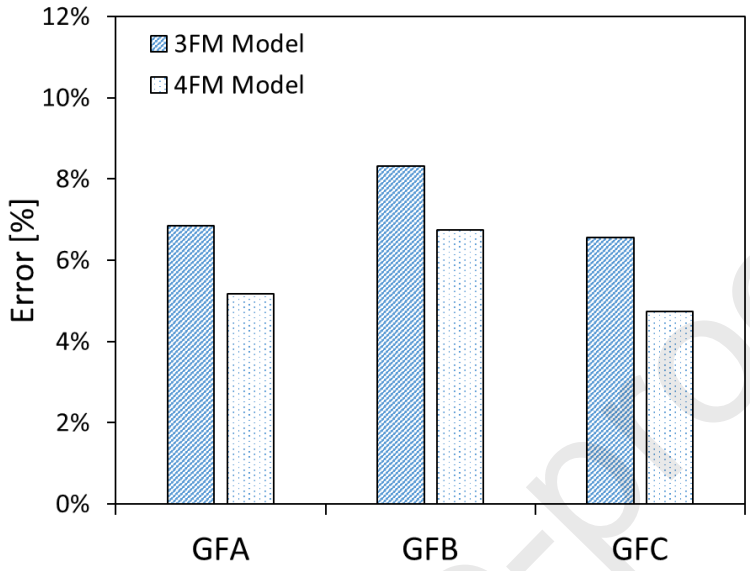

Figure 9. Forecasting P_{max} error of 3FM and 4FM models on hybrid composite laminate batches at different ageing times

Figure 9 summarizes the average error (i.e., defined as difference in percentage between theoretical and experimental maximum load, $(P_{model}-P_{exp})/P_{exp}$) obtained by comparing experimental data and theoretical Pmax predicted by 3FM or 4FM model. It is worth noting that the 4FM model shows a better reliability in comparison to 3FM model both on unaged and on aged conditions, showing an average error in the range 5-6%. This means that the proposed predictive model, although simplified, allows a coarse forecast of the pinned laminate resistance. Furthermore, this allows to predict, indicatively, the joint resistance reduction at increasing ageing time exposition. Overall, this model can be considered a suitable tool to perform a semi-quantitative evaluation of the mechanical performance variation of pinned joints induced by ageing.

A global view of the forecasting capabilities of the proposed Four Failure Mechanism Model can be observed in *Figure 10* in which the comparison between experimental P_{max} values of GFC batch, (i.e., aged for 60 days in the salt-fog spray chamber) with the theoretical model was shown. A quite good agreement between experimental data and the theoretical model in a wide range of E/D and W/D ratios can be noticed from this graph. The variation of the mechanical properties due to salt-fog exposition are taken into account with good approximation by the adopted approach, thus allowing to acquire an adequate determination of the mechanical durability of the pinned hybrid glass-flax joint.

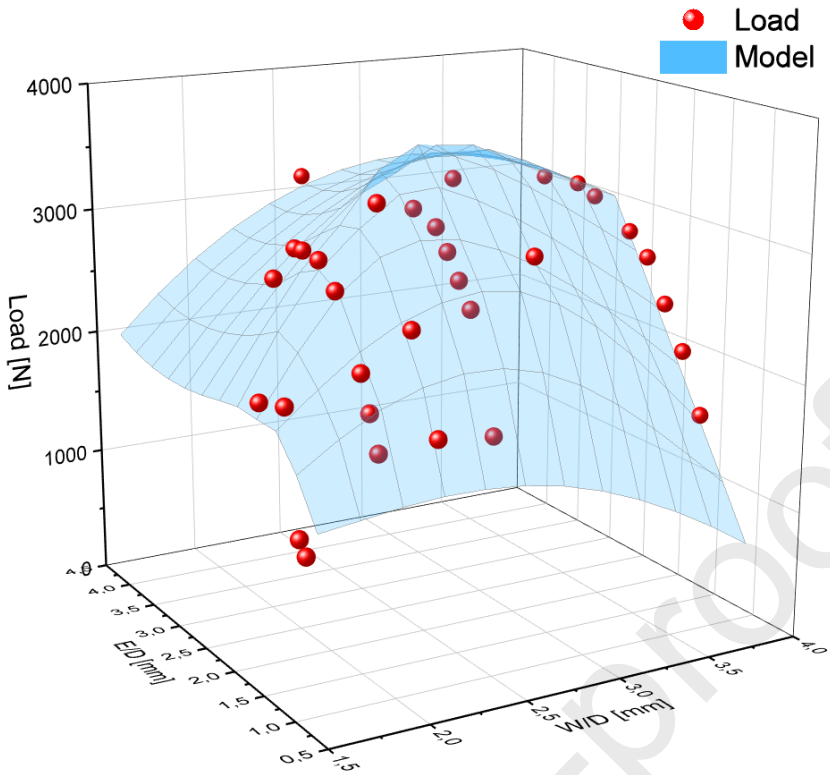

Figure 10. 3D plot of experimental maximum load data (red sphere markers) and forecasting Four Failure Mechanism Model (light blue surface)

The aim of this simplified approach is preliminarily the assessment of the maximum load reduction on single-pin laminates induced by the ageing condition. This approach is also able roughly to discriminate the competing failure phenomena. These results indicate that this model can be considered as valid and suitable design tool for a simplified study of the mechanical joints stability during life-time of composite structures. The present approach, if properly optimized, would allow to define intuitively the possible structural risks that could arise following prolonged exposure in an aggressive environment, such as salt-fog environment. This would make possible to guarantee targeted design constrain. At the same time, it entails the possibility to define preventive inspection procedures, thus limiting the risks of unexpected catastrophic damage of the structural components. Obviously, a more detailed analysis should be required to understand better the pin/hole stress modifications induced by local degradation phenomena also predicting quantitatively the critical failure load of the joint at varying geometry configurations, giving a further relevant improvement of knowledge on this topic.

Conclusions

This paper is focused on the evaluation of the predictive capabilities of a simplified theoretical approach on the mechanical behavior of aged pinned hybrid glass-flax composite laminates. The experimental results of the double-lap tests performed on unaged and aged in salt-fog environment (i.e., up to 60 days,) pinned samples were used as input data. In particular, in order to assess the predictive capability of the model in different joint and environmental configurations, the relationship among mechanical behavior, joint geometrical configuration and ageing time was investigated. Based on experimental results, a simplified theoretical approach was proposed to predict bearing load and failure mechanism occurrence at varying exposition time in salt-fog environment. No relevant modification on failure mechanism were identified comparing unaged and aged conditions. Furthermore, the results highlight that a reduction of maximum load, compared to unaged batch, was identified for long salt-fog exposition time. Depending on occurring failure mechanisms, specific geometrical joint configuration can be more sensitivity to salt-fog exposition. The model highlights a good reliability, with an average error of about 6-8% compared to experimental results. This means that the proposed methodology can be considered as a suitable approach to support the joining design of aged pinned composite laminates.

References

[1] Sarasini F, Fiore V. A systematic literature review on less common natural fibres and their biocomposites. J Clean Prod 2018;195:240–67. doi:10.1016/j.jclepro.2018.05.197.

[2] Singh J, Kumar M, Kumar S, Mohapatra SK. Properties of Glass-Fiber Hybrid Composites: A Review. Polym - Plast Technol Eng 2017;56:455–69. doi:10.1080/03602559.2016.1233271.

[3] Mahir FI, Keya KN, Sarker B, Nahiun KM, Khan RA. A brief review on natural fiber used as a replacement of synthetic fiber in polymer composites. Mater Eng Res 2019;1:88–99. doi:10.25082/mer.2019.02.007.

[4] Shishesaz M, Hosseini M. A review on stress distribution, strength and failure of bolted composite joints. J Comput Appl Mech 2018;49:415–29. doi:10.22059/jcamech.2018.269612.342.

[5] Khashaba UA, Sebaey TA, Alnefaie KA. Failure and reliability analysis of pinned-joints composite laminates: Effects of stacking sequences. Compos Part B Eng 2013;45:1694–703. doi:10.1016/j.compositesb.2012.09.066.

[6] Choudhury MR, Debnath K. Experimental analysis of tensile and compressive failure load in single-lap bolted joint of green composites. Compos Struct 2019;225:111180. doi:10.1016/j.compstruct.2019.111180.

[7] Abdullah MS, Abdullah AB, Samad Z. Structural integrity assessment of a composite joint: A review. Hole-Making Drill. Technol. Compos., Elsevier; 2019, p. 31–46. doi:10.1016/b978-0-08-102397-6.00003-9.

[8] Portemont G, Berthe J, Deudon A, Irisarri FX. Static and dynamic bearing failure of carbon/epoxy composite joints. Compos Struct 2018;204:131–41. doi:10.1016/j.compstruct.2018.07.069.

[9] Feng NL, Malingam SD, Irulappasamy S. Bolted joint behavior of hybrid composites. Fail. Anal. Biocomposites, Fibre-Reinforced Compos. Hybrid Compos., Elsevier; 2018, p. 79–95. doi:10.1016/B978-0-08-102293-1.00004-8.

[10] Bodjona K, Lessard L. Hybrid bonded-fastened joints and their application in composite structures: A general review. J Reinf Plast Compos 2016;35:764–81. doi:10.1177/0731684415627296.

[11] Rod Martin. Ageing of Composites | ScienceDirect. New York (USA): Woodhead Publishing Limited; 2008.

[12] Sahu SK, Rath MK. Hygrothermal Aging Behavior of Fiber-Reinforced Composites. Process. Green Compos., Singapore: Springer; 2019, p. 49–64. doi:10.1007/978-981-13-6019-0_4.

[13] Srinivasababu N. Understanding the durability of long sacred grass/Imperata cylindrica natural/hybrid FRP composites. Durab. Life Predict. Biocomposites, Fibre-Reinforced Compos. Hybrid Compos., Amsterdam: Elsevier; 2018, p. 300. doi:10.1016/B978-0-08-102290-0.00012-X.

[14] Son HG, Park Y Bin, Kweon JH, Choi JH. Fatigue behaviour of metal pin-reinforced composite single-lap joints in a hygrothermal environment. Compos Struct 2014;108:151–60. doi:10.1016/j.compstruct.2013.09.012.

[15] Choi J Il, Hasheminia SM, Chun HJ, Park JC, Chang HS. Failure load prediction of composite bolted joint with clamping force. Compos Struct 2018;189:247–55. doi:10.1016/j.compstruct.2018.01.037.

[16] Thoppul SD, Finegan J, Gibson RF. Mechanics of mechanically fastened joints in polymer-matrix composite structures - A review. Compos Sci Technol 2009;69:301–29. doi:10.1016/j.compscitech.2008.09.037.

[17] Li HS. Maximum entropy method for probabilistic bearing strength prediction of pin joints in composite laminates. Compos Struct 2013;106:626–34. doi:10.1016/j.compstruct.2013.05.040.

[18] Yang B, Yue Z, Geng X, Guan X, Wang P. Experimental and numerical study on bearing failure of countersunk composite–composite and composite–steel joints. J Compos Mater 2017;51:3211–24. doi:10.1177/0021998316684936.

[19] Lu F, Cai D, Tang J, Li W, Deng J, Zhou G. Bearing failure of single-/double-shear composite bolted joints: An explicit finite element modeling. J Reinf Plast Compos 2018;37:933–44. doi:10.1177/0731684418772355.

[20] Olmedo A, Santiuste C, Barbero E. An analytical model for predicting the stiffness and strength of pinned-joint composite laminates. Compos Sci Technol 2014;90:67–73. doi:10.1016/j.compscitech.2013.10.014.

[21] Sharos PA, Egan B, McCarthy CT. An analytical model for strength prediction in multi-bolt composite joints at various loading rates. Compos Struct 2014;116:300–10. doi:10.1016/j.compstruct.2014.05.021.

[22] Shamaei-Kashani AR, Shokrieh MM. An analytical approach to predict the mechanical behavior of single-lap single-bolt composite joints reinforced with carbon nanofibers. Compos Struct 2019;215:116–26. doi:10.1016/j.compstruct.2019.02.055.

[23] Xu P, Zhou Z, Liu T, Tan X, Pan S. A novel double-spring analytical model for hybrid GLARE joints: Model development, validation, parameter study and global sensitivity analysis. Int J Mech Sci 2020;177:105606. doi:10.1016/j.ijmecsci.2020.105606.

[24] Kradinov V, Madenci E, Ambur DR. Combined in-plane and through-the-thickness analysis for failure prediction of bolted composite joints. Compos Struct 2007;77:127–47. doi:10.1016/j.compstruct.2005.06.008.

[25] Camanho PP, Matthews FL. A Progressive Damage Model for Mechanically Fastened Joints in Composite Laminates. J Compos Mater 1999;33:2248–80. doi:10.1177/002199839903302402.

[26] Khashaba UA, Sebaey TA, Selmy AI. Experimental verification of a progressive damage model for composite pinned-joints with different clearances. Int J Mech Sci 2019;152:481–91. doi:10.1016/j.ijmecsci.2019.01.023.

[27] Sayman O, Ozen M, Sen F, Benli S. Sea water effect on failure behaviour of mechanically fastened composites. Mater Test 2013;55:349–54. doi:10.3139/120.110451.

[28] Karakuzu R, Kanlioğlu H, Deniz ME. Effect of seawater on pin-loaded laminated composites. Mater Test 2018;60:85–92. doi:10.3139/120.111121.

[29] Örçen G, Gür M, Özen M. Seawater effect on pin-loaded laminated composites with two parallel holes. J Mech Sci Technol 2012;26:4055–63. doi:10.1007/s12206-012-0909-2.

[30] Esendemir Ü, Cabioğlu AM. Investigating bearing strength of pin-loaded composite plates in different environmental conditions. J Reinf Plast Compos 2013;32:1685–97. doi:10.1177/0731684413500858.

[31] Örçen G, Gür M, Turan K. Progressive failure analysis on two parallel pinned joint glass/epoxy composite plates under the effect of seawater. J Compos Mater 2014;48:3499–511. doi:10.1177/0021998313510541.

[32] Calabrese L, Fiore V, Bruzzaniti P, Scalici T, Valenza A. Pinned hybrid glass-flax composite laminates aged in salt-fog environment: Mechanical durability. Polymers (Basel) 2020;12. doi:10.3390/polym12010040.

[33] Aktaş A, Uzun I. Sea water effect on pinned-joint glass fibre composite materials. Compos Struct 2008;85:59–63. doi:10.1016/j.compstruct.2007.10.007.

[34] Zhang J, Rowland J. Damage modeling of carbon-fiber reinforced polymer composite pin-joints at extreme temperatures. Compos Struct 2012;94:2314–25. doi:10.1016/j.compstruct.2012.03.011.

[35] Calabrese L, Fiore V, Bruzzaniti PG, Scalici T, Valenza A. An Aging Evaluation of the Bearing Performances of Glass Fiber Composite Laminate in Salt Spray Fog Environment. Fibers 2019;7:96. doi:10.3390/fib7110096.

[36] Fiore V, Calabrese L, Scalici T, Valenza A. Evolution of the bearing failure map of pinned flax composite laminates aged in marine environment. Compos Part B Eng 2020;187:107864. doi:10.1016/j.compositesb.2020.107864.

[37] Fiore V, Calabrese L, Scalici T, Bruzzaniti P, Valenza A. Bearing strength and failure behavior of pinned hybrid glass-flax composite laminates. Polym Test 2018;69:310–9. doi:10.1016/j.polymertesting.2018.04.041.

[38] Hossain MK, Chowdhury MMR, Imran KA, Salam MB, Tauhid A, Hosur M, et al. Effect of low velocity impact responses on durability of conventional and nanophased CFRP composites exposed to seawater. Polym Degrad Stab 2014;99:180–9. doi:10.1016/j.polymdegradstab.2013.11.008.

[39] Fang Y, Wang K, Hui D, Xu F, Liu W, Yang S, et al. Monitoring of seawater immersion degradation in glass fibre reinforced polymer composites using quantum dots. Compos Part B Eng 2017;112:93–102. doi:10.1016/j.compositesb.2016.12.043.

[40] Yan L, Chouw N. Effect of water, seawater and alkaline solution ageing on mechanical properties of flax fabric/epoxy composites used for civil engineering applications. Constr Build Mater 2015;99:118–27. doi:10.1016/j.conbuildmat.2015.09.025.

[41] Živković I, Fragassa C, Pavlović A, Brugo T. Influence of moisture absorption on the impact properties of flax, basalt and hybrid flax/basalt fiber reinforced green composites. Compos Part B Eng 2017;111:148–64. doi:10.1016/j.compositesb.2016.12.018.

[42] Pani PR, Nayak RK, Routara BC, Sekhar PC. Flexural and specific wear rate of seawater aged bamboo, jute and glass fiber reinforced polymer hybrid composites. Mater. Today Proc., vol. 18, Elsevier Ltd; 2019, p. 3409–14. doi:10.1016/j.matpr.2019.07.268.

[43] Afshar A, Liao HT, Chiang F pen, Korach CS. Time-dependent changes in mechanical properties of carbon fiber vinyl ester composites exposed to marine environments. Compos Struct 2016;144:80–5. doi:10.1016/j.compstruct.2016.02.053.

[44] Fiore V, Sanfilippo C, Calabrese L. Influence of sodium bicarbonate treatment on the aging resistance of natural fiber reinforced polymer composites under marine environment. Polym Test 2019;80:106100. doi:10.1016/j.polymertesting.2019.106100.

[45] Okutan B, Karakuzu R. The Failure Strength for Pin-Loaded Multi-Directional Fiber-Glass Reinforced Epoxy Laminate. J Compos Mater 2002;36:2695–712. doi:10.1177/002199802761675502.

[46] Fiore V, Calabrese L, Scalici T, Bruzzaniti P, Valenza A. Experimental design of the bearing performances of flax fiber reinforced epoxy composites by a failure map. Compos Part B Eng 2018;148:40–8. doi:10.1016/j.compositesb.2018.04.044.

[47] Malmstein M, Chambers AR, Blake JIR. Hygrothermal ageing of plant oil based marine composites. Compos Struct 2013;101:138–43. doi:10.1016/j.compstruct.2013.02.003.

[48] Wei B, Cao H, Song S. Degradation of basalt fibre and glass fibre/epoxy resin composites in seawater. Corros Sci 2011;53:426–31. doi:10.1016/j.corsci.2010.09.053.

[49] Paturel A, Dhakal HN. Influence of Water Absorption on the Low Velocity Falling Weight Impact Damage Behaviour of Flax/Glass Reinforced Vinyl Ester Hybrid Composites. Molecules 2020;25:278. doi:10.3390/molecules25020278.

[50] Akil HM, Cheng LW, Mohd Ishak ZA, Abu Bakar A, Abd Rahman MA. Water absorption study on pultruded jute fibre reinforced unsaturated polyester composites. Compos Sci Technol 2009;69:1942–8. doi:10.1016/j.compscitech.2009.04.014.

[51] Fiore V, Calabrese L, Di Bella G, Scalici T, Galtieri G, Valenza A, et al. Effects of aging in salt spray conditions on flax and flax/basalt reinforced composites: Wettability and dynamic mechanical properties. Compos Part B Eng 2016;93:35–42. doi:10.1016/j.compositesb.2016.02.057.

[52] Thuault A, Eve S, Blond D, Bréard J, Gomina M. Effects of the hygrothermal environment

on the mechanical properties of flax fibres. J Compos Mater 2014;48:1699–707. doi:10.1177/0021998313490217.

[53] Assarar M, Scida D, El Mahi A, Poilâne C, Ayad R. Influence of water ageing on mechanical properties and damage events of two reinforced composite materials: Flax-fibres and glass-fibres. Mater Des 2011;32:788–95. doi:10.1016/j.matdes.2010.07.024.

[54] Baley C, Le Duigou A, Bourmaud A, Davies P. Influence of drying on the mechanical behaviour of flax fibres and their unidirectional composites. Compos Part A Appl Sci Manuf 2012;43:1226–33. doi:10.1016/j.compositesa.2012.03.005.

[55] Bos HL, Van Den Oever MJA, Peters OCJJ. Tensile and compressive properties of flax fibres for natural fibre reinforced composites. J Mater Sci 2002;37:1683–92. doi:10.1023/A:1014925621252.

[56] Mohanty AK, Misra M, Hinrichsen G. Biofibres, biodegradable polymers and biocomposites: An overview. Macromol Mater Eng 2000;276–277:1–24. doi:10.1002/(SICI)1439-2054(20000301)276:1<1::AID-MAME1>3.0.CO;2-W.

[57] Dhakal HN, Zhang ZY, Richardson MOW. Effect of water absorption on the mechanical properties of hemp fibre reinforced unsaturated polyester composites. Compos Sci Technol 2007;67:1674–83. doi:10.1016/j.compscitech.2006.06.019.

[58] Calabrese L, Fiore V, Scalici T, Valenza A. Experimental assessment of the improved properties during aging of flax/glass hybrid composite laminates for marine applications. J Appl Polym Sci 2019;136:47203. doi:10.1002/app.47203.

[59] Shin PS, Kim JH, Park HS, Baek YM, Lee S Il, DeVries KL, et al. A Review: Mechanical and Interfacial Properties of Composites after Diverse Types of Aging Using Micromechanical Evaluation. Fibers Polym 2020;21:225–37. doi:10.1007/s12221-020-9700-7.

[60] Malmstein M, Chambers AR, Blake JIR. Hygrothermal ageing of plant oil based marine composites. Compos Struct 2013;101:138–43. doi:10.1016/j.compstruct.2013.02.003.

[61] Fiore V, Calabrese L, Proverbio E, Passari R, Valenza A. Salt spray fog ageing of hybrid composite/metal rivet joints for automotive applications. Compos Part B Eng 2017. doi:10.1016/j.compositesb.2016.09.096.

[62] Awadhani L V., Bewoor AK. Analytical and experimental investigation of Effect of

geometric parameters on the failure modes in a single lap single bolted metal to GFRP composite bolted joints subjected to axial tensile loading. Mater. Today Proc., 2017. doi:10.1016/j.matpr.2017.07.063.

[63] Ahmad H, Crocombe AD, Smith PA. Strength prediction in CFRP woven laminate bolted single-lap joints under quasi-static loading using XFEM. Compos Part A Appl Sci Manuf 2014. doi:10.1016/j.compositesa.2014.07.013.

[64] Valenza A, Fiore V, Borsellino C, Calabrese L, Di Bella G. Failure Map of Composite Laminate Mechanical Joint. J Compos Mater 2007;41:951–64. doi:10.1177/0021998306067257.

[65] Calabrese L, Fiore V, Scalici T, Bruzzaniti P, Valenza A. Failure maps to assess bearing performances of glass composite laminates. Polym Compos 2019;40:1087–96. doi:10.1002/pc.24806.

[66] Fiore V, Sanfilippo C, Calabrese L. Dynamic Mechanical Behavior Analysis of Flax/Jute Fiber-Reinforced Composites under Salt-Fog Spray Environment. Polymers (Basel) 2020;12:716. doi:10.3390/polym12030716.

[67] Di Bella G, Calabrese L. Pin-Contact Behaviour of Composite Sandwich Structures Under Compressive Bearing Load. Appl Compos Mater 2011;18:197–210. doi:10.1007/s10443-010-9146-y.

[68] Li H, Zhang K, Cheng H, Suo H, Cheng Y, Hu J. Multi-stage mechanical behavior and failure mechanism analysis of CFRP/Al single-lap bolted joints with different seawater ageing conditions. Compos Struct 2019;208:634–45. doi:10.1016/j.compstruct.2018.10.044.

[69] Qiu C, Guan Z, Du S, Li Z, Huang Y. Prediction of the net-tension strength of single bolt joint using the 0° ply strength and fracture toughness. Compos Part B Eng 2019;161:386–94. doi:10.1016/j.compositesb.2018.12.053.

[70] Chamis CC. Simplified Composite Procedures for Designing Bolted Joints, NASA Technical Memorandum 100281. 1988.

Vincenzo Fiore: Methodology, Data curation, Writing- Original draft preparation, Reviewing and Editing. **Luigi Calabrese:** Conceptualization, Methodology, Investigation, Data curation, Reviewing and Editing.